

Correlation functions of cold bosons in an optical lattice

Radka Bach¹ and Kazimierz Rzażewski^{1,2}¹*Center for Theoretical Physics, Polish Academy of Sciences, al. Lotników 32/46, 02-668 Warsaw, Poland*²*Faculty of Mathematics and Sciences, Cardinal Stefan Wyszyński University, al. Lotników 32/46, 02-668 Warsaw, Poland*

(Received 7 June 2004; published 30 December 2004)

Motivated by the experimental observation of collapses and revivals of Bose matter wave field, we investigate correlation functions of cold bosons in an optical lattice. Within a simple model we examine two kinds of states: one that employs the commonly used notion of coherent states, and one that obeys the total number of atoms conservation. We identify rare situations at which these states behave differently. Typically, however, their predictions coincide and so: As a function of “interaction time” the interference pattern in the density undergoes collapse and revival. Exactly at revival times the system mimics the ideal gas case, in which all correlation functions factorize, while in the collapsed phase of the evolution the system effectively behaves as if initially there was no long-range coherence. Even in the latter case though, an interference pattern should be seen in a single experiment. We stress the role of column averaging, which in fact corresponds to an averaged observation of an ensemble of two-dimensional realizations. We also note that, contrary to the common belief, an interference pattern should also be seen in a single observation of a Mott state.

DOI: 10.1103/PhysRevA.70.063622

PACS number(s): 03.75.Lm

I. INTRODUCTION

Cold bosons in optical lattices have gained a lot of attention recently because of the ease and precision with which they can be manipulated [1]. For example, it was an optical lattice that enabled the observation of collapses and revivals of a matter wave field [2]. Even though the theoretical analysis of this experiment provided by authors is based on the notion of coherent states and as such is—in principle, at least—inadequate to describe systems with total number of atoms fixed, it seems to work quite well. It is our purpose to describe this experiment more accurately, in particular to examine the role of total number of atoms conservation and identify situations in which it will clearly manifest itself.

This will be achieved with the aid of correlation functions. Contrary to the common belief, there is no need to build a separate experimental setup to measure higher-order correlation functions in atomic systems—it is enough to analyze photographs of a cloud of atoms. Such photographs, which are typically obtained in the final stage of experiments with cold gases, are nothing else but a simultaneous detection of many atoms and therefore probe the correlation function of the order of the number of atoms [3]. And since the observed system comprises of a fixed number of atoms, it is described by a Fock state; consequently it is possible to reconstruct low-order correlation functions out of these measurements [4]. Having the possibility of measuring correlation functions, it is justified to investigate them theoretically as well.

The article is organized as follows. In Sec. II we start with a brief description of the experiment in which collapses and revivals of a matter wave field were observed. On this basis two states of the system are introduced: one that obeys the total number of atom conservation and one that violates it (the latter for comparison). Correlation functions corresponding to both states are calculated and investigated in Sec. III. Inter alia, we identify situations in which predictions of the two examined states differ. We also note that in the collapsed

phase the system effectively behaves as if there was no site-to-site coherence, as pointed out in Sec. IV. Even then, though, the second-order correlation function shows non-trivial structure and interference pattern should be seen in a single photograph. Counterintuitively, this is also the case for Mott insulator, as shown in Sec. V, and it is extremely difficult to tell these states apart on the basis of a single or many measurements. We conclude in Sec. VI.

II. THE EXPERIMENT

The experiment in which collapses and revivals of the matter wave field were observed [2] was composed of a few steps. After preparing a Bose-Einstein condensate in a harmonic oscillator potential, an optical lattice potential was slowly raised. The height of this lattice has been chosen such that the system was still completely in the superfluid regime. Then, the intensity of light creating the lattice was rapidly increased and the resulting optical lattice was so high that the tunneling between the sites was strongly suppressed. Was this raising done adiabatically, the system would move to the Mott insulating phase; but because it was done rapidly, the atom number distribution at each well from a superfluid state was preserved at the high lattice potential, thus producing a mixture of Fock states with different number of atoms at each well. The system was then left to evolve for some time, which was varied from experiment to experiment (we will call it interaction time and denote T). Finally, after switching off all potentials the atomic cloud was allowed to expand freely for time t before shooting a photograph. As a function of the interaction time T a collapse and a revival of the interference pattern were seen.

We are going to describe this experiment via a simple model which nonetheless includes the most relevant features of the system. For example, we will neglect the nonuniformity of the optical lattice stemming from additional harmonic oscillator potentials (one used to create the Bose-

Einstein condensate and another one associated with widths of laser beams), but consider a system composed of \mathcal{N} atoms distributed among \mathcal{K} equivalent lattice sites instead. The notion of atom density, $\rho = \mathcal{N}/\mathcal{K}$, will be used interchangeably. The wells' exact shape is also not important since we are going to assume that atoms are so cold that they do not have enough energy to occupy states other than the ground state, which is justified by the fact that the most important part of the evolution—the one from which collapses and revivals stem—takes place when lattice potential is very high and when the energy of an atom is far less than the energy gap to the first excited state.

Prior to turning on the strong optical lattice the system was in a superfluid state and so right after raising the potential the distribution of atoms between wells is multinomial. Hence the state of the system is

$$|\psi(T=0)\rangle = \sqrt{\frac{\mathcal{N}!}{\mathcal{K}^{\mathcal{N}}}} \sum_{n_1=0}^{\mathcal{N}} \sum_{n_2=0}^{\mathcal{N}} \cdots \sum_{n_{\mathcal{K}}=0}^{\mathcal{N}} \underbrace{1}_{\substack{\text{total number of atoms} \\ \text{conservation law}}} |n_1, n_2, \dots, n_{\mathcal{K}}\rangle, \quad (1)$$

where the under-brace denotes total number of atoms conservation law, i.e., $n_1 + n_2 + \cdots + n_{\mathcal{K}} = \mathcal{N}$ and we have already assumed that each atom can occupy any of the wells with equal probability.

Once prepared, the system is left to evolve for time T . Since atoms are now imprisoned in a strong optical lattice in which tunneling is highly suppressed, in each well they evolve independently of others. Assuming contact interactions between atoms, the Hamiltonian in each well is effectively of the form:

$$\hat{H} = \frac{\hbar g}{2} \hat{n}(\hat{n} - 1), \quad (2)$$

where \hat{n} is the operator of the number of atoms in this well and g denotes the rescaled coupling constant:

$$g = \frac{4\pi\hbar a}{m} \int d\mathbf{x} |\varphi(\mathbf{x})|^4 \quad (3)$$

[$\varphi(\mathbf{x})$ is the wave function of the ground state of a well and a is the s -wave scattering length]. Then, after time T the state of the system is

$$|\psi_{\text{mmmm}}(T)\rangle = \sqrt{\frac{\mathcal{N}!}{\mathcal{K}^{\mathcal{N}}}} \sum_{n_1=0}^{\mathcal{N}} \sum_{n_2=0}^{\mathcal{N}} \cdots \sum_{n_{\mathcal{K}}=0}^{\mathcal{N}} \underbrace{1}_{\substack{\text{total number of atoms} \\ \text{conservation law}}} \times c_{n_1}(T) \cdots c_{n_{\mathcal{K}}}(T) |n_1, n_2, \dots, n_{\mathcal{K}}\rangle, \quad (4)$$

where the coefficients $c_n(T)$ are

$$c_n(T) = \frac{1}{\sqrt{n!}} \exp\left\{-i\frac{gT}{2}n(n-1)\right\}. \quad (5)$$

To investigate the role of total number of atoms conservation law, however, we are going to analyze a coherent counterpart of this state as well:

$$|\psi_{\text{coh}}(T)\rangle = e^{-\rho\mathcal{K}/2} \sum_{n_1=0}^{\infty} \sum_{n_2=0}^{\infty} \cdots \sum_{n_{\mathcal{K}}=0}^{\infty} \alpha^{n_1+n_2+\cdots+n_{\mathcal{K}}} \times c_{n_1}(T) \cdots c_{n_{\mathcal{K}}}(T) |n_1, n_2, \dots, n_{\mathcal{K}}\rangle, \quad (6)$$

where the coefficients $c_n(T)$ are defined as before and $|\alpha|^2 = \rho$ for consistency.

As far as a subsystem composed of a fixed number of wells is concerned, the multinomial state approaches the coherent one when the number of atoms and the number of wells are increased in such a way that the density is kept constant.¹ In this limit—let us call it thermodynamic limit in analogy with statistical mechanics—the remaining part of the system serves as a particle reservoir and not surprisingly the distribution of atoms factorizes and becomes poissonian in each well independently, as it is for coherent states.

It is also worth noting that the presented model does not account for possible effects associated with the reduced dimensionality of atoms confined in the optical lattice, for example it is not applicable to systems in strongly-interacting Tonks-Girardeau regime (see [5] for discussion of correlation functions in this particular case).

III. CORRELATION FUNCTIONS

Let us now calculate explicit analytic formulas for correlation functions for the multinomial and coherent state introduced above. The r th order correlation function is defined as

$$G^{(r)}(\mathbf{x}_1, \mathbf{x}_2, \dots, \mathbf{x}_r; T, t) = \langle \psi(T) | \hat{\Psi}^\dagger(\mathbf{x}_1, t) \cdots \hat{\Psi}^\dagger(\mathbf{x}_r, t) \hat{\Psi}(\mathbf{x}_r, t) \cdots \hat{\Psi}(\mathbf{x}_1, t) | \psi(T) \rangle. \quad (7)$$

In the above formula two distinct times appeared: the interaction time T , denoting how long atoms were left to evolve in the strong optical lattice potential, and the measurement time, t , which is the time between switching off all binding potentials and shooting the actual photograph. During the latter time there are no external potentials and we also assume that the interaction does not play any major role—consequently the only effect this process has on the system is the free expansion of wells' wave functions. Although this way the interaction phases that atoms might have acquired are neglected, the assumption is not only justified (since during expansion the system becomes extremely dilute), but it also clarifies the overall picture. Each of the times is now responsible for different physical effects: the interaction time, T , governs the phases of different Fock states and therefore is responsible for collapses and revivals, while the measurement time, t , determines the behavior of wells' wave functions and as such does not influence the relation between different Fock states. Note also that the time t is treated here rather as a convenient control parameter than a true argument of the correlation function.

The field operator $\hat{\Psi}(\mathbf{x}, t)$ can be decomposed in any complete basis of annihilation operators. In the system we are

¹At least from the point of view of the correlation functions we are investigating.

considering it is convenient to introduce annihilation operators of atoms at individual sites' ground states: $\hat{\Psi}(\mathbf{x}, t) = \sum_{k=1}^{\mathcal{K}} \varphi_k(\mathbf{x}, t) \hat{a}_k$. Then after some lengthy though straightforward calculations one obtains

$$G^{(r)}(\mathbf{x}_1, \dots, \mathbf{x}_r; T, t) = \rho^r \sum_{l_1, \dots, l_r} \sum_{k_1, \dots, k_r} \omega(\{l, k\}, T) \times \varphi_{l_1}^*(\mathbf{x}_1, t) \cdots \varphi_{l_r}^*(\mathbf{x}_r, t) \varphi_{k_1}(\mathbf{x}_1, t) \cdots \varphi_{k_r}(\mathbf{x}_r, t), \quad (8)$$

where

$$\omega_{\text{coh}}(\{l, k\}, T) = \mathcal{R}(\{l, k\}, T) \exp\{\rho \mathcal{Q}(\{l, k\}, T)\} \quad (9)$$

for coherent states and

$$\omega_{\text{mnm}}(\{l, k\}, T) = \frac{\mathcal{N}!}{\mathcal{N}^r (\mathcal{N} - r)!} \mathcal{R}(\{l, k\}, T) \left(1 + \frac{\mathcal{Q}(\{l, k\}, T)}{\mathcal{K}}\right)^{\mathcal{N} - r} \quad (10)$$

for multinomial states. The functions \mathcal{R} and \mathcal{Q} are

$$\mathcal{R}(\{l, k\}, T) = \exp\left\{i \frac{gT}{2} \sum_{i=1}^{\mathcal{K}} \left[\left(\sum_{j=1}^r \delta_{l_j, i} \right)^2 - \left(\sum_{j=1}^r \delta_{k_j, i} \right)^2 \right]\right\}, \quad (11a)$$

$$\mathcal{Q}(\{l, k\}, T) = \sum_{i=1}^{\mathcal{K}} (e^{igT \sum_{j=1}^r (\delta_{l_j, i} - \delta_{k_j, i})} - 1). \quad (11b)$$

First of all the expression for the correlation does not depend on the interaction time T nor the coupling strength g alone, but on the product of the two. It means that at $T=0$ the interacting system effectively mimics the behavior of an ideal gas, for which, as can be easily checked, all correlation functions factorize (for multinomial states there appears an additional proportionality constant). And because the functions \mathcal{R} and \mathcal{Q} are periodic functions of gT , this also happens for any time such that $gT=2k\pi$, where k is an integer. This reappearance of the interference pattern is nothing else but the revival phenomenon.

A. The first-order correlation function

Density—the first-order correlation function—is obtained from above formulas via setting $r=1$ and can be written as

$$G^{(1)}(\mathbf{x}) = \rho \sum_k |\varphi_k(\mathbf{x})|^2 + \kappa \rho \sum_l \sum_{k \neq l} \varphi_l^*(\mathbf{x}) \varphi_k(\mathbf{x}), \quad (12)$$

where

$$\kappa = \begin{cases} \exp\left\{-4\rho \sin^2\left(\frac{gT}{2}\right)\right\} & \text{for coherent states,} \\ \left[1 - \frac{4}{\mathcal{K}} \sin^2\left(\frac{gT}{2}\right)\right]^{\mathcal{N}-1} & \text{for multinomial states.} \end{cases} \quad (13)$$

First of all, the density is a sum of two kinds of terms: the background, which is a simple consequence of having on

average ρ atoms at each lattice site, and interference terms. The presence and relative amplitude of the latter is governed by the coefficient κ .

To observe interference pattern two conditions must be simultaneously fulfilled: (i) the interaction time gT is such that the coefficient κ is not vanishing and (ii) the measurement time, t , is such that the wave functions $\varphi_i(\mathbf{x})$ substantially overlap. The latter condition controls the exact shape of interference pattern observed while the first one influences its visibility. To compare predictions of multinomial versus coherent states it is therefore enough to investigate the coefficient κ only. It is astonishing how quickly—when increasing the number of wells—predictions of the two states coincide: practically from 3 wells upwards there is no way to distinguish multinomial from coherent states through density profiles. Only for two wells, $\mathcal{K}=2$, is there a substantial discrepancy: binomial distribution predicts an additional revival at $gT=\pi$. Interesting enough, the interference pattern observed at this additional revival is in-phase with the pattern at $gT=0$ for odd number of atoms and out-of-phase for even number of atoms. One might think that investigating the situation with only two wells is pushing the analysis beyond the limits set by experimental reality. This is not true, however. Only slight modification of the experiment is required to go into this interesting regime.² Imagine that before the first optical lattice (the one, in which the atomic system is in a superfluid state) is turned on, another optical lattice is raised: a lattice deep enough to force the system into the Mott insulator state, with a well defined number of atoms per site. Let us now turn on a lattice with half the spatial period of the one already existing: this will produce a binomial distribution of atoms in each deep potential well between two shallow wells.

The vanishing of the coefficient κ for almost all interaction times apart from the ones close to revival times is the origin of the collapse phenomenon. To estimate the time of collapse T^* one can require the coefficient κ to reach a preset small value, ϵ . Then

$$\cos(gT_{\text{mnm}}^*) \leq 1 - \frac{\mathcal{K}}{2} (1 - \epsilon^{1/(\mathcal{N}-1)}), \quad (14a)$$

$$\cos(gT_{\text{coh}}^*) \leq 1 + \frac{\ln \epsilon}{2\rho}. \quad (14b)$$

Note that the collapse is (apart from $\mathcal{K}=2, 3$ cases) never exact, i.e., when demanding the interference fringes to vanish completely, which corresponds to setting $\epsilon=0$, the above inequalities cannot be satisfied. At least not without simultaneously increasing the density ρ . However, for any practical purposes it is enough to have the visibility of fringes smaller than the sensitivity of detectors to speak about complete collapse of interference pattern. For multinomial distributions of atoms among small number of wells, on the other hand, there exist interaction times for which fringes vanish identically: these are $gT_{\text{mnm}}^* = \frac{1}{4} \times 2\pi$ and $gT_{\text{mnm}}^* = \frac{3}{4} \times 2\pi$ for $\mathcal{K}=2$ case,

²This idea originates from private communication with Immanuel Bloch.

and $gT_{\text{minn}}^* = \frac{1}{3} \times 2\pi$ and $gT_{\text{minn}}^* = \frac{2}{3} \times 2\pi$ for $\mathcal{K}=3$ case.

B. The second-order correlation function

Let us concentrate on the normalized second order correlation function, defined as

$$g^{(2)}(\mathbf{x}, \mathbf{x}') = \frac{G^{(2)}(\mathbf{x}, \mathbf{x}')}{G^{(1)}(\mathbf{x})G^{(1)}(\mathbf{x}')} \quad (15)$$

because this way information about the density is set aside and only correlations are being investigated. For interaction time such that $gT=2k\pi$, where $k=0, 1, 2, \dots$, i.e., exactly the revival time, the normalized second-order correlation function is constant, because then the ideal gas case is recovered and consequently

$$g_{gT=2k\pi}^{(2)}(\mathbf{x}, \mathbf{x}') = \begin{cases} 1 & \text{for coherent state,} \\ 1 - \frac{1}{\mathcal{N}} & \text{for multinomial state.} \end{cases} \quad (16)$$

Already, there is a difference between the two states examined: multinomial states predict a small antibunching effect, $g^{(2)}(\mathbf{x}, \mathbf{x}') < 1$, which is due to the total number of atoms conservation law: the chance of detecting an atom at position \mathbf{x} is smaller if another atom was already detected somewhere else (than if it was not) because there are fewer atoms altogether. Note that this result will hold also for other interaction times, provided \mathbf{x} and \mathbf{x}' are distant enough.

However, if one moves away from the exact revival time, so that gT is no longer an integer multiple of 2π , it is practically impossible to get any insight into the behavior of the physical system analytically—by investigating the formulas alone, especially with arbitrary wave functions $\varphi_i(\mathbf{x})$. Therefore, we have chosen to investigate the system via numerical simulations of one-dimensional lattices, varying the number of lattice sites, the atom density and the width of the initial wave packet (which, in our simple model, corresponds to the height of the optical lattice). In the simulations we put the wells' centers on the net with spacing equal to 1, so the unit of length is simply half the wavelength of light used to create an optical lattice potential. Prior to the switching off the lattice, wave packets were Gaussians located at the center of the corresponding lattice site: $\varphi_i(x, t=0) \propto \exp(-(x-x_i)^2/2\sigma^2)$, where x_i is the location of the center of the i th well, σ denotes the Gaussian's width and the proportionality constant includes normalization factor, but the phases of all wave functions are set identical. The expansion of the field operator, $\hat{\Psi}$, as a sum of annihilation operators of atoms at ground states of different lattice sites implicitly assumes that these wave functions form an orthogonal set. Although this condition cannot be perfectly fulfilled for any set of Gaussian wave packets, the overlap of wave functions of adjacent sites is $\exp(-\sigma^{-2})$ and consequently it can be made arbitrarily small by decreasing σ . In the actual simulations σ was varied between 0.03 and 0.12, which yields nonorthogonalities between 10^{-480} and 10^{-31} . (The experimental value of σ in [2] translated to the system of units adopted here was around 0.15.) As explained before, wave packets were allowed to expand freely for time t before taking the measurement.

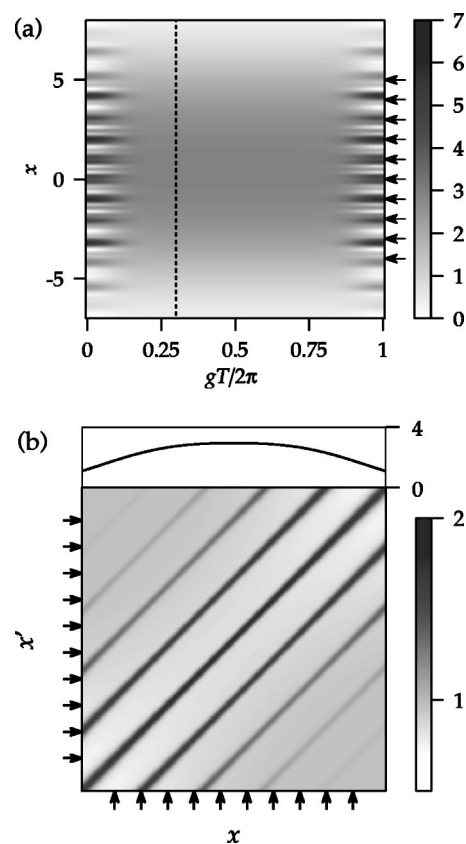


FIG. 1. First- and second-order correlation functions for one-dimensional system composed of $\mathcal{K}=10$ wells and $\mathcal{N}=30$ atoms. The wells' wave functions were Gaussians of initial width, $\sigma=0.12$, and the measurement time was $t=3\sigma$. Arrows denote the positions of wells' centers. (a) Density profiles versus the interaction time, gT . Both the collapse and the revival of interference pattern is clearly visible. (b) Close-up for a certain value of interaction time, $gT=0.3 \times 2\pi$. The curve at the top is the density profile (this is a cut along the dotted line from the figure above). The two-dimensional density plot denotes the normalized second-order correlation function, $g^{(2)}(x, x')$.

Time is measured in units $m\lambda^2/(4\hbar)$, where m is the mass of an atom while λ denotes the wavelength of light used to create the optical lattice potential. In these units the density of a single wave packet after expansion is just a Gaussian of width given by $\sqrt{\sigma^2 + (t/\sigma)^2}$. For large measurement times it is therefore convenient to express t as multiples of the initial width, σ , because then it is clear over how many sites the wave packet has spread. For example, a measurement time $t=4\sigma$ means that each wave packet “probes” roughly a sphere of radius 4, i.e., 4 lattice sites in each direction.

For interaction times T different from revival times the results of simulations are the following: First of all, $g^{(2)}(x, x')$ correlation function exhibits a structure. Typically, these are diagonal stripes in the $x-x'$ plane, such that the normalized second order correlation function depends only on the difference of its spatial arguments: $g^{(2)}(x, x') \approx g^{(2)}(x-x')$, as seen at Fig. 1(b) (at least far from the boundaries of the system). It means that in every realization interference fringes are going to be observed, but the whole pattern will move from shot to shot and will vanish after averaging, pro-

ducing a smooth density profile. Secondly, the range of $g^{(2)}$ is closely related to the size of expanding wave packets (which depends on the measurement time, t). Speaking roughly, to have a nontrivial correlation, wave packets must spread over the distance equal to the separation between the points at which $g^{(2)}$ is calculated or measured. The separation between the fringes, on the other hand, is determined by the initial size of expanding wave packets, or, in other words, by the momenta involved: the steeper the optical lattice potential, the more localized the wave function and the more fringes in the second-order correlation function structure.

The formulas for correlation functions are quite distinct for both kinds of states, it is thus somewhat surprising that the predictions obtained in numerical simulations are practically indistinguishable. To spot possible discrepancies we have investigated coefficients $\omega(\{l, k\})$ defined by Eq. (8) in more detail, and found that even though these coefficients depend on four indices, they can take only one of six values (this happens—technically speaking—because functions \mathcal{R} and \mathcal{Q} depend not on the values of the indices themselves, but on their mutual relation, i.e., on the way they split into equivalence classes with respect to the number of identical values). In the limit $\mathcal{K} \rightarrow \infty$ and $\mathcal{N} \rightarrow \infty$ such that $\rho = \mathcal{N}/\mathcal{K} = \text{const}$, the coefficients corresponding to multinomial states become identical with the ones stemming from coherent states, which is yet another manifestation of the equivalence of the two states in the thermodynamic limit. This limit is achieved so quickly that from $\mathcal{K}=5$ upwards there is practically no way of distinguishing between the two states.³ Only for $\mathcal{K}=2, 3, 4$ wells case is there a room for discrepancies and indeed such situations in one-dimensional case are found and depicted in Fig. 2. Apart from optical lattices there exists a number of experimental techniques used in atom interferometry that can create potentials comprised of a few wells, for example atom chip devices [6,7] or optical tweezer systems [8,9].

The conclusions presented above—stemming from one-dimensional simulations—are not altered when extending the analysis to higher dimensions. With one important note, however. The structure in the second-order correlation function implies that interference pattern should be seen in every single realization and smooth out when averaged over many experiments, producing a relevant density profile. This is true for a measurement which detects atoms in the full, 3-dimensional physical space and is in general false for its 2-dimensional projection (think about holograms versus photographs). The latter is governed by a column-averaged correlation function, in which information about correlations in the direction of the illuminating light pulse is lost, and such a situation corresponds to performing many 2-dimensional experiments and averaging over them. This explains why the collapse was seen at all in a single experimental run. Numerical simulations of a lattice composed of 5×5 sites show that the visibility of the interference pattern drops from 44% when averaged over one layer to 19% when averaged over all 5 layers, and the effect is expected to be even more profound for larger systems.

³Provided that the density is not extremely low, i.e., the number of atoms, \mathcal{N} , is at least of order 10 rather than of order 1.

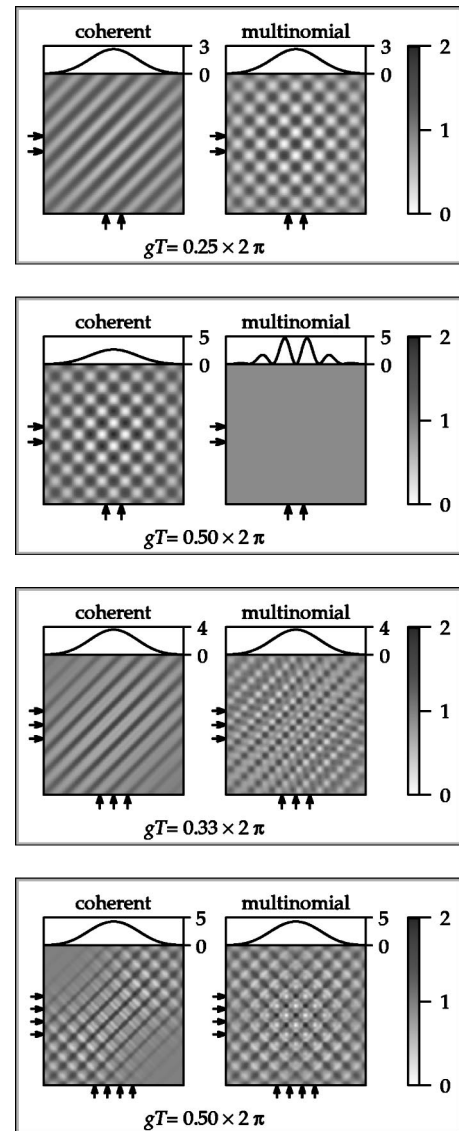


FIG. 2. Situations, at which coherent and multinomial states give distinctively different predictions. Density plots denote the normalized second-order correlation function, $g^{(2)}(x, x')$, where x and x' are on the horizontal and vertical axis, respectively. Arrows denote the position of the wells' centers. One-dimensional graph on top of the density plot is the density, $G^{(1)}(x)$. The parameters of physical systems, apart from the number of wells and the interaction time, are identical for all plots: atom density, $\rho=5$, measurement time, $t=2\sigma$, and initial width of expanding wave packets, $\sigma=0.12$.

IV. INCOHERENT SYSTEMS

The system examined herein before was implicitly assumed to be perfectly coherent, in a sense that in numerical simulations wave functions of all optical lattice sites had identical phases. This was because in the experimental situation the system prior to the turning on the strong optical lattice potential was in a superfluid phase, which exhibits long-range coherence. However, in principle, the same formalism is also applicable to the situation in which there is no long-range coherence in the initial state, i.e., the wave func-

tions' phases are completely random. Even though the physical relevance of such a state might be questionable, it is worth to examine this limit as well, because then one could separate effects originating from having a mixture of Fock states at each site from the ones necessarily requiring the coherence between sites. The state with completely random phases is also interesting because—at least when large measurement times are concerned—it can be to a large extent investigated analytically independently of its size and dimension.

Let us therefore assume that (i) the wave functions of individual wells have random phases: $\varphi_k(\mathbf{x}) \rightarrow e^{i\phi_k} \varphi_k(\mathbf{x})$, where ϕ_k are random numbers between 0 and 2π , and (ii) the measurement time t is so large that at each point in space wave functions of many sites overlap. Then, in the expressions for the first- and second-order correlation functions all terms that explicitly depend on phases ϕ_k will average out, producing

$$\overline{G^{(1)}}(\mathbf{x}) = \rho \sum_k |\varphi_k(\mathbf{x})|^2, \quad (17a)$$

$$\begin{aligned} \overline{G^{(2)}}(\mathbf{x}, \mathbf{x}') &= \omega_0 \overline{G^{(1)}}(\mathbf{x}) \overline{G^{(1)}}(\mathbf{x}') \\ &+ \omega_0 \rho^2 \sum_l \sum_{k \neq l} \varphi_l^*(\mathbf{x}) \varphi_k(\mathbf{x}) \varphi_l(\mathbf{x}') \varphi_k^*(\mathbf{x}'), \end{aligned} \quad (17b)$$

where $\omega_0 = 1$ for coherent and $1 - 1/\mathcal{N}$ for multinomial states.

Note that these expressions do not depend upon the interaction time at all. Therefore the fact that the experimentally observed pattern changed with interaction time is a clear sign of the coherence in the initial state. The density shows no interference pattern and is exactly the same as the one of system with coherence in the collapsed phase, i.e., when κ in Eq. (12) is close to zero. Note however that here the mechanism is intrinsically different: The interference pattern is absent not because of the collapse of the matter wave field at each individual well, but because of the washing-out effect when overlapping subsystems with different phases. If one looked at a single well subsystem, one would have seen collapses and revivals there, just as it was pointed out in the first article concerning this phenomenon in Bose-Einstein condensates [10].

The second-order correlation function, on the other hand, shows additional structure, which depends on the overlap of wells wave functions, $\varphi_l^*(\mathbf{x}) \varphi_k(\mathbf{x})$. If the measurement time is large enough this function is just a smooth profile modulated by a spatially-dependent phase of the form $\exp(i\mathbf{p}\mathbf{x})$, where \mathbf{p} is related to initial widths of expanding wave packets, and then the pattern observed in the second-order correlation function comprises of diagonal stripes in the $\mathbf{x} - \mathbf{x}'$ hyperplane, just as the ones seen at Fig. 1(b). The fact that in the collapsed phase of the evolution systems with perfect coherence have practically the same first- and second-order correlation functions as systems with completely random phases implies that it is impossible to distinguish between them, neither in a single nor many experiments. In that sense one

could say that in the collapsed phase the system with long-range coherence mimics the behavior of the system with no coherence at all.

The difference between multinomial and coherent states manifests itself only in the coefficient ω_0 (1 versus $1 - 1/\mathcal{N}$), which leads to a small antibunching effect, as also seen in the case of systems with perfect coherence. Similarly, the structure in the second-order correlation function vanishes when column averaged. This is a consequence of the fact that the free evolution propagator acts independently in each direction. Initially the wave functions were very well localized at different points in space and therefore their product vanished identically: $\varphi_l^*(\mathbf{x}, t=0) \varphi_k(\mathbf{x}, t=0) \approx 0$. Therefore, column averaging at the initial instant—which is nothing else but integrating this product over one coordinate—yields zero. This is also true for any measurement time t because such an averaged expression is nothing else but a scalar product and as such cannot be changed during a unitary evolution. (Note that this reasoning requires that the projection of the whole evolution operator onto one dimensional subspace determined by the direction of propagation of the illuminating light needs still to be unitary, which is true for free evolution but not in general.)

V. MOTT INSULATOR

For comparison let us also investigate an ideal Mott insulator, i.e., a state with the same number of atoms in each well:

$$|\psi_{\text{Mott}}\rangle = |\rho, \rho, \dots, \rho\rangle, \quad (18)$$

where ρ is now an integer (and naturally it is still the density of an atomic sample). The achievement of the Mott phase is probably the most important experimental result with cold atoms in optical lattices [11]. Correlation functions in such a system are straightforward to calculate

$$G_{\text{Mott}}^{(1)}(\mathbf{x}) = \rho \sum_k |\varphi_k(\mathbf{x})|^2, \quad (19a)$$

$$\begin{aligned} G_{\text{Mott}}^{(2)}(\mathbf{x}, \mathbf{x}') &= \rho(\rho - 1) \sum_k |\varphi_k(\mathbf{x})|^2 |\varphi_k(\mathbf{x}')|^2 \\ &+ \rho^2 \sum_{k \neq l} |\varphi_k(\mathbf{x})|^2 |\varphi_l(\mathbf{x}')|^2 \\ &+ \rho^2 \sum_l \sum_{k \neq l} \varphi_l^*(\mathbf{x}) \varphi_k(\mathbf{x}) \varphi_l(\mathbf{x}') \varphi_k^*(\mathbf{x}'). \end{aligned} \quad (19b)$$

These formulas bear a close resemblance to Eqs. (17) and therefore the predictions are quite similar as well. In particular, even in a Mott insulating phase one is going to observe interference pattern in a single measurement, because its second-order correlation function exhibits the striped structure. The only difference between the Mott insulator and a state with mixture of Fock states with random phases (or with coherence but in a collapsed phase of the evolution) lies in the first term in the Eq. (19b). Consequently, to distinguish between these states one should perform a measurement with

very short measurement times, so that the overlap of wave functions of adjacent sites is vanishing, and look at the diagonal part of the second-order correlation function only, which will be $G^{(2)}(\mathbf{x}, \mathbf{x}) = \omega_0 \rho^2 \sum_k |\varphi_k(\mathbf{x})|^4$ for states with mixtures of Fock states at each site and $G_{\text{Mott}}^{(2)}(\mathbf{x}, \mathbf{x}) = \rho(\rho - 1) \sum_k |\varphi_k(\mathbf{x})|^4$ for Mott insulator. Note that the difference is the most significant for systems with low densities, in particular $G_{\text{Mott}}^{(2)}(\mathbf{x}, \mathbf{x})$ vanishes identically if $\rho = 1$.

The second-order correlation function for a Mott insulating phase was already theoretically investigated in [12]. Moreover, recently a high-contrast matter wave interference between 30 independent Bose-Einstein condensates released from a one-dimensional optical lattice was indeed observed experimentally [13]. The visibility of the interference pattern in a single experiment was similar both for phase-correlated condensates and for phase-uncorrelated condensates. In an earlier experiment of this kind [14], the interference pattern was only observed when atoms were released from a shallow optical lattice and it was almost completely lost when the lattice depth was increased. These two results seem to contradict each other, but a closer analysis shows this is not the case. The reason for different observations lies mostly in the particular choice of the measurement time, i.e., how long it took between switching off the potentials and taking the image of the expanded cloud of atoms. To see this let us compare correlation functions of two extremes: a Mott state and a coherent state. After the expansion the density of a Mott state is just a Gaussian, while for coherent states the density comprises of interference spikes modulated by a Gaussian envelope. Let us denote the ratio of the latter Gaussian envelope to the density of a Mott state by η . In the simplest case this will be $\eta = \max\{G_{\text{coh}}^{(1)}(\mathbf{x})\} / \max\{G_{\text{Mott}}^{(1)}(\mathbf{x})\}$. As far as the second-order correlation function is concerned, for a Mott state an interference pattern cannot become arbitrarily large. In the best possible case all “interfering” terms in the Eq. (19b) contribute in-phase, which in turn yields the maximum value of the second-order correlation function twice the uncorrelated background: $\max\{G_{\text{Mott}}^{(2)}(\mathbf{x}, \mathbf{x}')\} = 2(\max\{G_{\text{Mott}}^{(1)}(\mathbf{x})\})^2$. Correlation functions for coherent states, on the other hand, factorize and therefore the second-order correlation function is just a product of the densities, hence: $\max\{G_{\text{coh}}^{(2)}(\mathbf{x}, \mathbf{x}')\} = (\max\{G_{\text{coh}}^{(1)}(\mathbf{x})\})^2$. Therefore, the ratio of maximum values of the second-order correlation functions for coherent states and for a Mott state, $\max\{G_{\text{coh}}^{(2)}\} / \max\{G_{\text{Mott}}^{(2)}\} = \eta^2/2$. In the experiment [13] the ex-

pansion time was relatively short yielding $\eta \approx 3$ and the resulting ratio in the second-order correlation function is around 4.5. For the experiment [14], on the other hand, expansion time was very long, such that $\eta = 11.7$ and the maximum of the second-order correlation function was 70 times smaller than its coherent counterpart and could have easily dropped below the resolution of the imaging system. Of course this analysis does not pretend to describe any of these experiments quantitatively, but it shows where the reason for observed discrepancies most likely lies.

VI. CONCLUSIONS

We have investigated the recent experiment of collapses and revivals of the matter wave field in terms of correlation functions. We show that exactly at revival times an interacting system mimics the behavior of an ideal gas and all correlation functions factorize. In the collapsed phase of the evolution, on the other hand, the system effectively behaves as if there was no coherence between the sites of the optical potential. This does not imply, however, that a smooth density is obtained in a single realization of the experiment: on the contrary, we show that the second-order correlation function exhibits structure and therefore interference pattern should be seen in a single measurement. Counterintuitively, the same conclusions hold also for the Mott insulating phase, which has already been proven experimentally.

The fact that the collapse of the matter wave field was seen experimentally at all is due to the column averaging. We stress the difference between a result of a single measurement and a column averaged single measurement (the latter corresponds in fact to a measurement averaged over an ensemble of two-dimensional experiments). We also show how to differentiate between the different states via a single measurement.

We investigate the role of the total number of atoms conservation. In particular we identify rare situations in which predictions of multinomial and coherent states differ. Unsurprisingly, they all correspond to situations with small number of lattice sites.

ACKNOWLEDGMENTS

We would like to thank I. Bloch for his useful comments. The work was partially supported by the Subsidy of the Foundation for Polish Science and by the Polish Ministry of Scientific Research and Information Technology under Grant No. PBZ-MIN-008/P03/2003.

[1] See, for example, I. Bloch, *Phys. Today* **17**(4), 25 (2004).
 [2] M. Greiner, O. Mandel, T. W. Hansch, and I. Bloch, *Nature (London)* **419**, 51 (2002).
 [3] J. Javanainen and S. M. Yoo, *Phys. Rev. Lett.* **76**, 161 (1996).
 [4] R. Bach and K. Rzażewski, *Phys. Rev. Lett.* **92**, 200401 (2004).
 [5] D. M. Gangardt, P. Pedri, L. Santos, and G. V. Shlyapnikov, e-print cond-mat/0408437.

[6] E. A. Hinds, C. J. Vale, and M. G. Boshier, *Phys. Rev. Lett.* **86**, 1462 (2001).
 [7] W. Hänsel, J. Reichel, P. Hommelhoff, and T. W. Hänsch, *Phys. Rev. A* **64**, 063607 (2001).
 [8] G. Reymon, N. Schlosser, I. Protchenko, and P. Grangier, *Philos. Trans. R. Soc. London, Ser. A* **361**, 1527 (2003).
 [9] Y. Shin, M. Saba, T. A. Pasquini, W. Ketterle, D. E. Pritchard, and A. E. Leanhardt, *Phys. Rev. Lett.* **92**, 050405 (2004).

- [10] E. M. Wright, D. F. Walls, and J. C. Garrison, *Phys. Rev. Lett.* **77**, 2158 (1996).
- [11] M. Greiner, O. Mandel, T. Esslinger, T. W. Hänsch, and I. Bloch, *Nature (London)* **415**, 39 (2002).
- [12] E. Altman, E. Demler, and M. D. Lukin, *Phys. Rev. A* **70**, 013603 (2004).
- [13] Z. Hadzibabic, S. Stock, B. Battelier, V. Bretin, and J. Dalibard, e-print quant-ph/0405113.
- [14] C. Orzel, A. K. Tuchman, M. L. Fenselau, M. Yasuda, and M. A. Kasevich, *Science* **291**, 2386 (2001).